Icarus 308 (2018) 188–196

Contents lists available at ScienceDirect

Icarus

journal homepage: www.elsevier.com/locate/icarus

Seasonal variability in winds in the north polar region of Mars

Isaac B. Smith[a,*], Aymeric Spiga[b]

[a] Planetary Science Institute, 1546 Cole Blvd Suite 120, Denver, CO 80204, USA
[b] Laboratoire de Météorologie Dynamique (LMD/IPSL), Sorbonne Universités, UPMC Univ Paris 06, PSL Research University, Ecole Normale Supérieure, Université Paris-Saclay, École Polytechnique, Centre National de la Recherche Scientifique France, France

ARTICLE INFO

Article history:
Received 2 March 2017
Revised 19 September 2017
Accepted 3 October 2017
Available online 5 October 2017

ABSTRACT

Surface features near Mars' polar regions are very active, suggesting that they are among the most dynamic places on the planet. Much of that activity is driven by seasonal winds that strongly influence the distribution of water ice and other particulates. Morphologic features such as the spiral troughs, Chasma Boreale, and prominent circumpolar dune fields have experienced persistent winds for several Myr. Therefore, detailing the pattern of winds throughout the year is an important step to understanding what processes affect the martian surface in contemporary and past epochs. In this study, we provide polar-focused mesoscale simulations from northern spring to summer to understand variability from the diurnal to the seasonal scales. We find that there is a strong seasonality to the diurnal surface wind speeds driven primarily by the retreat of the seasonal CO_2 until about summer solstice, when the CO_2 is gone. The fastest winds are found when the CO_2 cap boundary is on the slopes of the north polar layered deposits, providing a strong thermal gradient that enhances the season-long katabatic effect. Mid-summer winds, while not as fast as spring winds, may play a role in dune migration for some dune fields. Late summer wind speeds pick up as the seasonal cap returns.

1. Introduction

Studies of the polar regions of Mars provide evidence of significant wind activity as wind streaks (Howard, 2000), volatile transport (Warner and Farmer, 2008), dune movement (Hansen et al., 2011), and spiral trough evolution (Howard et al., 1982; Smith and Holt, 2010; Smith et al., 2013,2014). The polar layered deposits (PLD) strongly interact with the atmosphere on diurnal, seasonal, and annual bases and are therefore considered to be among the most active places on the surface of Mars (Byrne, 2009; Hvidberg et al., 2012). Because of this activity, significant work has gone into understanding polar processes and evolution. Furthermore, recent observations have captured dune and ripple migration, allowing for measurements of mass flux and estimations on timing and magnitude of events (Ewing et al., 2010; Middlebrook, 2015), so comparisons with modeled wind directions and speeds are becoming a reliable test for thresholds of geomorphic activity.

Some of the greatest questions about the origin, onset, and development of the PLD, especially the north PLD (NPLD), have been answered by modeling (Levrard et al., 2007) and later supported with radar investigations (Putzig et al., 2009; Smith et al., 2016a). Levrard et al. (2007) focused on long-term evolution but left other interesting questions regarding the PLD morphology and current activity unanswered. To get a better understanding of the current processes, especially the volatile transport that shapes the NPLD and surrounding dune fields, seasonal studies using regional-scale (mesoscale) atmospheric modeling are required.

High-resolution atmospheric modeling offers the benefit of providing context for many processes, both above and at the surface, in our current situation of a relative paucity of polar observations on Mars. Based on more and more sophisticated physics and increasing computing power, modern models represent a breakthrough in our ability to describe the martian environment. The models, both Global Climate Models (GCMs) and mesoscale models, provide predictions for weather hazards and entry descent and landing, or study of the global water, dust, and CO_2 cycles. During the last several decades modeling skills have improved sufficiently along with increasing resolution and number of observations that they are now being used in complementary ways to study individual features or annual weather patterns.

With the increase in frequency and potency of models, many studies found success in answering limited questions by employing GCMs and mesoscale atmospheric models using boundary conditions from GCMs. Regarding polar weather and surface features, these investigations used techniques that fell into one of three categories: studies of small features at high temporal and spatial resolution (Fenton et al., 2014,2005); studies covering large areas

* Corresponding author.
E-mail address: ibsmith@psi.edu (I.B. Smith).

https://doi.org/10.1016/j.icarus.2017.10.005
0019-1035/

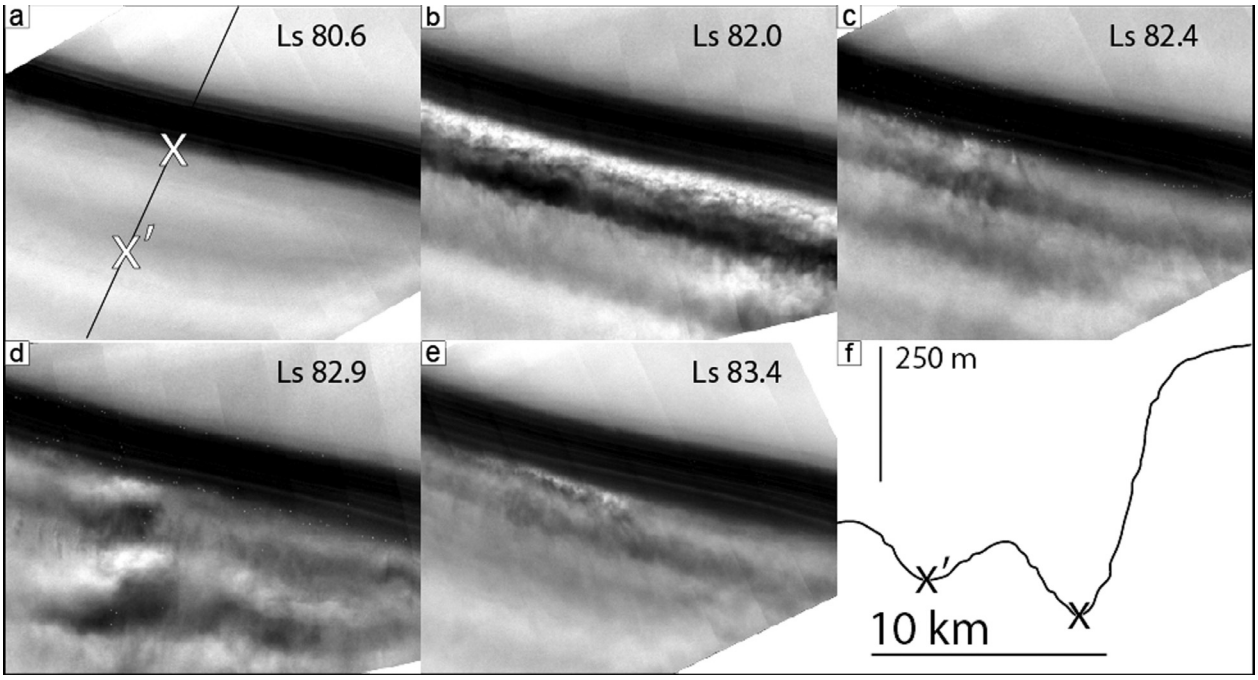

Fig. 1. Trough clouds seen at about 85° N, 90° E in a single martian year. (a) to (e) Thermal Emission Imaging System (THEMIS) images with same footprint: V28706003, V28744006, V28756004, V28769004, V28781003. Dates and scales listed. (f) Topographic profile of vertical line in (a). Xs mark the local minimum elevations in the imaged trough. Clouds are especially prominent in this region between L_s 80° and 83°.

over many dates but with low resolution (Hayward et al., 2007, 2009); and studies at high spatial resolution covering a large area but with limited date ranges (Tyler and Barnes, 2005, 2014). The benefit of these targeted studies is clear; each resulted in an answer that addressed a specific question regarding surface features or atmospheric observations. However, the narrow focus of each study fundamentally limited them to targeted investigations, and one cannot be applied to another.

Here we present a new approach that combines simulations over extensive date ranges with intermediate resolution, providing more context for atmosphere-surface interactions than previous targeted studies. Our product is a database of simulations useful for extracting wind speeds during a nominal day with diurnal circulation over large regions. In this study, we are able to readily extract seasonal wind speeds at specific locations in the northern polar region of Mars to determine which date ranges experience the greatest wind velocity. In the following sections we use this technique to compare the wind's influence on surface and atmospheric activity with our simulations.

2. Background

2.1. Polar processes

Many processes are proposed to explain the formation of the polar landscape, but, excluding impact related features, three stand out as the most likely: wind transport, atmospheric deposition of volatiles and dust, and sublimation. These processes are sufficient to explain the creation of large chasmae (Warner and Farmer, 2008; Holt et al., 2010), spiral troughs (Howard et al., 1982; Smith et al., 2013, 2014; Smith and Holt, 2010), large scours called "wirebrush terrain" (Koutnik et al., 2005), dune fields (Ewing et al., 2010), outlier deposits (Conway et al., 2012; Brothers et al., 2013), and surface streaks and various other surface features (Howard, 2000).

These three processes have the benefit of being observable directly from orbit and indirectly by monitoring surface changes. Wind transport leaves streaks on the surface and is responsible for moving ice from one side of a trough to the other (Howard, 2000; Smith et al., 2013). Direct detection of CO_2 and H_2O snowfall (Whiteway et al., 2009; Hayne et al., 2014), changes in elevation and mass (Smith et al., 2001), seasonal albedo variations of both PLD (Calvin and Titus, 2008), and atmospheric column abundances (Farmer and Doms, 1979) demonstrate the occurrence of seasonal deposition and sublimation. Of these processes, wind likely plays the most prominent role in creating the variability in landforms, as described from mapping based on observations of the Shallow Radar instrument (SHARAD) on Mars Reconnaissance Orbiter (Brothers et al., 2013, 2015; Holt et al., 2010; Smith and Holt, 2010, 2015). This is also true for dune fields, which respond much more quickly to winds (Bridges et al., 2012) than the larger, ice dominated PLD.

2.2. Katabatic jumps and trough clouds

Besides surface changes, the detection of atmospheric phenomena, such as clouds, attests to the potency of winds, sublimation, and deposition. In a pair of papers describing observations on both poles Smith et al. (2013, 2014) cataloged nearly 1000 clouds within the spiral troughs on both poles. The material that made up these clouds was interpreted to be water ice based on arguments of pressure and temperature, and the location of these clouds (parallel to and directly above the spiral depressions) indicated that wind, upslope sublimation, and downslope condensation into ice crystals control their formation (Fig. 1). The clouds were interpreted as Martian analogs to clouds that form on Earth at the site of katabatic jumps (Lied, 1964; Pettré and André, 1991). A katabatic jump is most concisely described as "a narrow zone with large horizontal changes in wind speed, pressure, and temperature," (Pettré and André, 1991). They are analogous to hydraulic jumps found at the bottom of waterfalls, in kitchen sinks, or in rivers (Fig. 15 from Smith et al., 2013).

The clouds that result from katabatic jumps are found just above the lowest portion of the spiral troughs (Fig. 1) because a

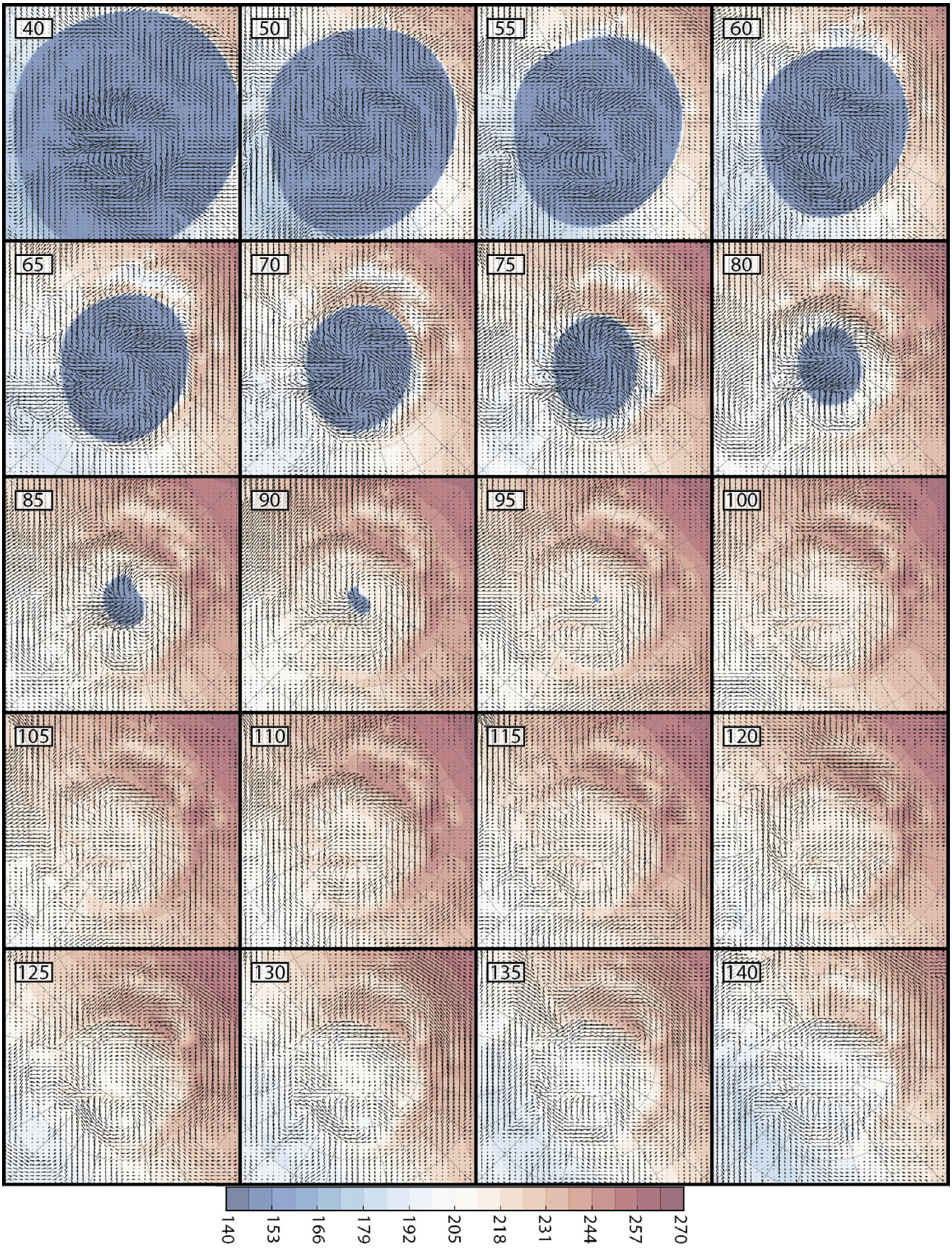

Fig. 2. Model output showing surface temperature (in K) and wind directions 20 m above the surface for most dates in our simulation (L_s 40°–140°). The CO_2 seasonal cap dominates the surface thermal environment, and thermal contrasts of 100 K sometimes appear over very short distances. After ~L_s 95° the seasonal cap disappears, and the surface winds are much weaker (Fig. 4).

rapid change in wind speed occurs at the change in slope near the lowers section. As wind enters the trough from upstream it accelerates, and a jump triggers when the slope changes direction (Figs. 15 from both Smith et al., 2013, 2014). Flow thickness often triples over a short distance, but wind velocities may decrease from as many as 20 m s^{-1} to as few as ~1 m s^{-1} (Spiga and Smith, this issue; Fig. 14 from Smith et al., 2013). With a sufficient amount of water vapor, these strong perturbations, especially those associated with temperature decrease and pressure increase, are sufficient to explain the formation of clouds. Very high-resolution simulations of katabatic winds are able to reproduce the katabatic jumps at precisely the same locations as the clouds are observed, giving great confidence that katabatic winds and jumps drive spiral trough evolution. For a dedicated discussion of this process see Spiga and Smith (this issue).

3. Mesoscale simulations

By mesoscale simulations, we refer to computer modeling of the atmospheric state (temperature, pressure, wind) on a specific region of interest on Mars, and evolution thereof over the course of three days (Michaels and Rafkin, 2008; Rafkin, 2009; Spiga et al., 2011; Spiga and Forget, 2009; Toigo et al., 2002; Tyler and Barnes, 2005, 2014). A mesoscale atmospheric model comprises two main parts: an hydrodynamical solver computing the dynamics of the atmospheric fluid at a given spatial resolution, coupled with physical packages describing the phenomena impacting this fluid below the resolved scales: e.g., radiative transfer, turbulent mixing, surface-atmosphere interactions. Mesoscale modeling is designed to compute the atmospheric state on a limited area with fine mesh spacing, as opposed to Global Climate Modeling which does so on the whole planet with coarse spatial resolution.

We carried out mesoscale simulations of the northern polar regions using the Laboratoire de Météorologie Dynamique (LMD) Martian Mesoscale Model (MMM) (Spiga and Forget, 2009). Our simulations were designed to cover latitudes pole-ward of 75° N with a resolution of ~18 km per cell and represent diurnal winds in the current climate. They were run for a duration of three days every 5° L_s from L_s 30° to 140°. Dates outside this range are also simulated, but as the seasonal CO_2 ice cap provides a physical barrier for winds interacting with the surface, we exclude them from this presentation. This setup provides context for the PLD and surrounding dune fields at sufficient resolution to gain knowledge about large-scale features (troughs and dune fields) and the diurnal to seasonal variability of winds that affect them. Atmospheric conditions at the boundary of the domain employed in the mesoscale simulations are imposed based on the LMD Mars GCM (Forget et al., 1999).

The simulations use polar stereographic projections, and physical parameterizations similar to the previous studies by Smith et al. (2013, 2014). The version of the MMM used in this study is close to the one used in Spiga et al. (2011) and Massé et al. (2012). Domain settings are analogous to the ones employed in Smith et al. (2013).

To model near-surface winds in the Martian polar regions, it is particularly important to account for the evolution of the seasonal CO_2 ice deposits (Siili et al., 1999; Toigo et al., 2002) because on CO_2 ice deposits, surface temperature is determined by the CO_2 gas-ice equilibrium temperature. For this purpose, we cannot rely on the CO_2 surface frost cover predicted by the coarse-resolution GCM. Instead, we use a prescribed CO_2 seasonal deposit that evolves by L_s date according to infrared measurements (from the Thermal Emission Spectrometer) of the surface temperature during three Mars years (24, 25, and 26) (Titus, 2005). This setup matches that of our previous study in the south (Smith et al., 2014), which permitted to conclude that the retreat of the seasonal CO_2 ice cap strongly affects the intensity of near-surface polar winds. Outside the seasonal CO_2 deposits, surface temperature is calculated in our model by a surface energy balance model (as in Spiga and Forget, 2009). We use the surface thermophysical properties (albedo and thermal inertia) suitable for northern polar regions used in the polar mesoscale model (Putzig et al., 2014; Tyler and Barnes, 2014).

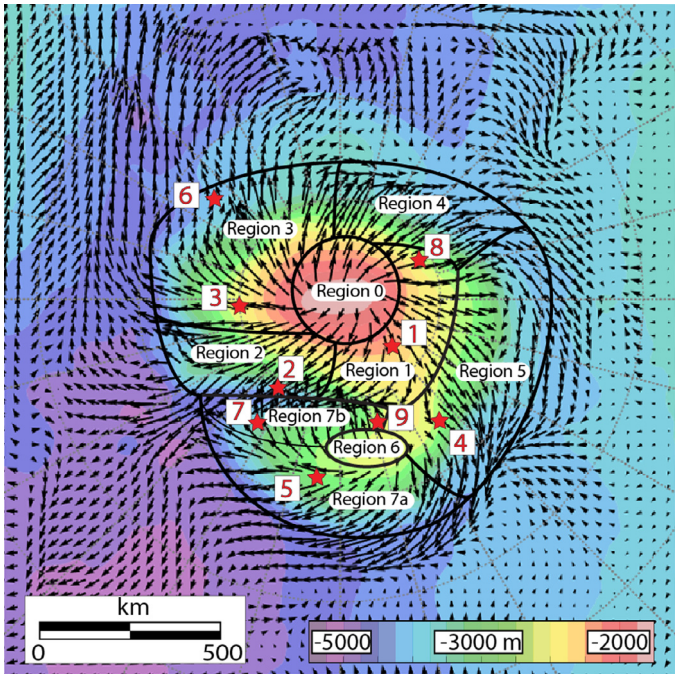

Fig. 3. Location map for wind speed extractions (Figs. 4 and 5) and regional boundaries ad defined by Smith and Holt (2015) on colorized topography. Coordinate for each location in Table 1.

Because the simulations only cover three days each, regional transients in polar regions described in Tyler and Barnes (2005) do not have sufficient time to develop. Those atmospheric phenomena also affect wind speeds and directions, and future work will study them, but the simulations we present here were aimed at characterizing the effects of diurnal winds and seasonal variability thereof.

4. Results and discussion

In our simulations, we were able to identify the direct effect that seasonal CO_2 ice has on wind speed and direction. This is especially important in late spring (Fig. 2, L_s 70–90°), when the seasonal CO_2 ice boundary is within the margin and on the slopes of the NPLD. At this time the winds have small diurnal variations inside the crocus line (external extent of the seasonal cap) but significant changes in speed and direction outside. This is further illustrated by a movie included in supplementary information.

The diurnal wind circulations are strongly controlled by the surface temperature contrasts. CO_2 covers the surface for part of the year setting the surface temperature at the sublimation temperature of ~145 K. Regions outside of the CO_2 boundary reach temperatures near the freezing point of water, nearly 130 K higher. This spatial boundary between where CO_2 is present and where the surface is uncovered expresses a discontinuous temperature. The strong contrast retreats poleward through the spring as the CO_2 cap retreats, and the fastest winds retreat poleward at the same rate (Fig. 2, Smith et al., 2014). To demonstrate this we plot the maximum and average simulated winds at nine locations for each simulated date (Fig. 4). Location coordinates can be found are

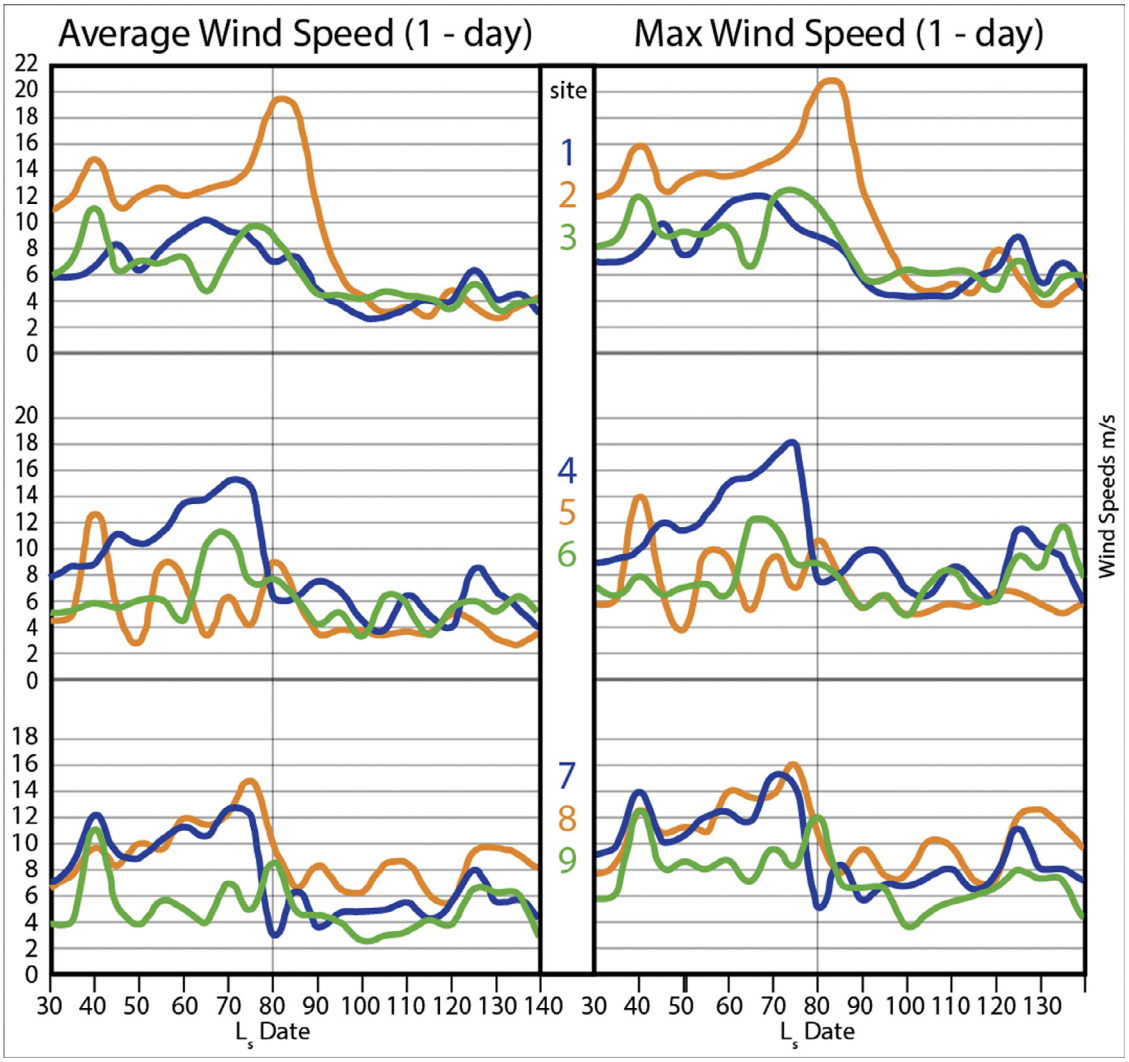

Fig. 4. Average and maximum regional wind speeds 20 m above the surface for the final day at each date of our simulation. Wind speeds pick up during spring, as the seasonal cap retreats (Fig. 2). After the crocus line passes each location the speeds drop by a factor of 2–5x. Locations match those in Fig. 3. The cause of the anomalously high wind speeds at L_s 40° are not explained in these simulations.

Table 1
Sites corresponding to locations indicated in Fig. 3.

	1	2	3	4	5	6	7	8	9
Lat (°N)	86°	86°	86°	82°	82°	82°	84°	84°	84°
Lon (°E)	70°	330°	260°	50°	0°	220°	330°	120°	30°

Table 1. Immediately apparent is that the intensity of the wind increases for all locations throughout spring until the seasonal cap retreats to higher latitudes. At that point the wind speed drops precipitously. Locations at higher latitudes retain the higher wind speeds for longer periods because the seasonal cap takes longer to reach them. Once the seasonal cap has completely disappeared, between L_s 95° and 100°, wind speeds at the NPLD are reduced for every location until later in the summer. This dominant seasonal effect is driven by two important factors. First, the thermal contrast between the CO_2 surface ice at the crocus line and the nearby uncovered ground (water ice or bedrock) can reach > 100 K (Smith et al., 2014, see also Toigo et al., 2002). This extreme temperature contrast reinforces an effect analogous to "sea breeze" on Earth that enhances surface winds in the direction of warmer surface temperatures (as in the case on a terrestrial beach). The second effect is that of katabatic winds near the slope of the NPLD. Katabatic winds are drainage winds that form when cold air resides near a sloping surface. The cold air is denser than the ambient air, and that density contrast drives the air mass to lower elevations, often straight down a slope with secondary steering directed by the Coriolis force, especially in the polar regions. The two effects work simultaneously, and horizontal wind speeds greater than 20 m s^{-1} are simulated in our highest resolution simulations (see Spiga and Smith this issue).

The seasonal simulations can be indirectly validated by orbital observations of clouds. Using the geologic regions of the NPLD delineated by Smith and Holt (2015) (Fig. 3), we are able to count the number of clouds that are detected in each region and compare that to the maximum wind speeds in the same region (Fig. 5). Compared to a null hypothesis that the clouds disappear after L_s 80°, we find that the number of detected clouds is maximum after that date for Regions 1–3, where the cloud counts drop at L_s 85° or 90° Regions 4 and 7a peak at around L_s 80° and Region 5 peaks before. No clouds have been detected in Regions 6 or 7b.

As a whole, wind speeds increase throughout spring, and cloud counts are reasonably correlated to that increase. Together, cloud count and wind speed drop precipitously soon after the seasonal cap retreats farther north.

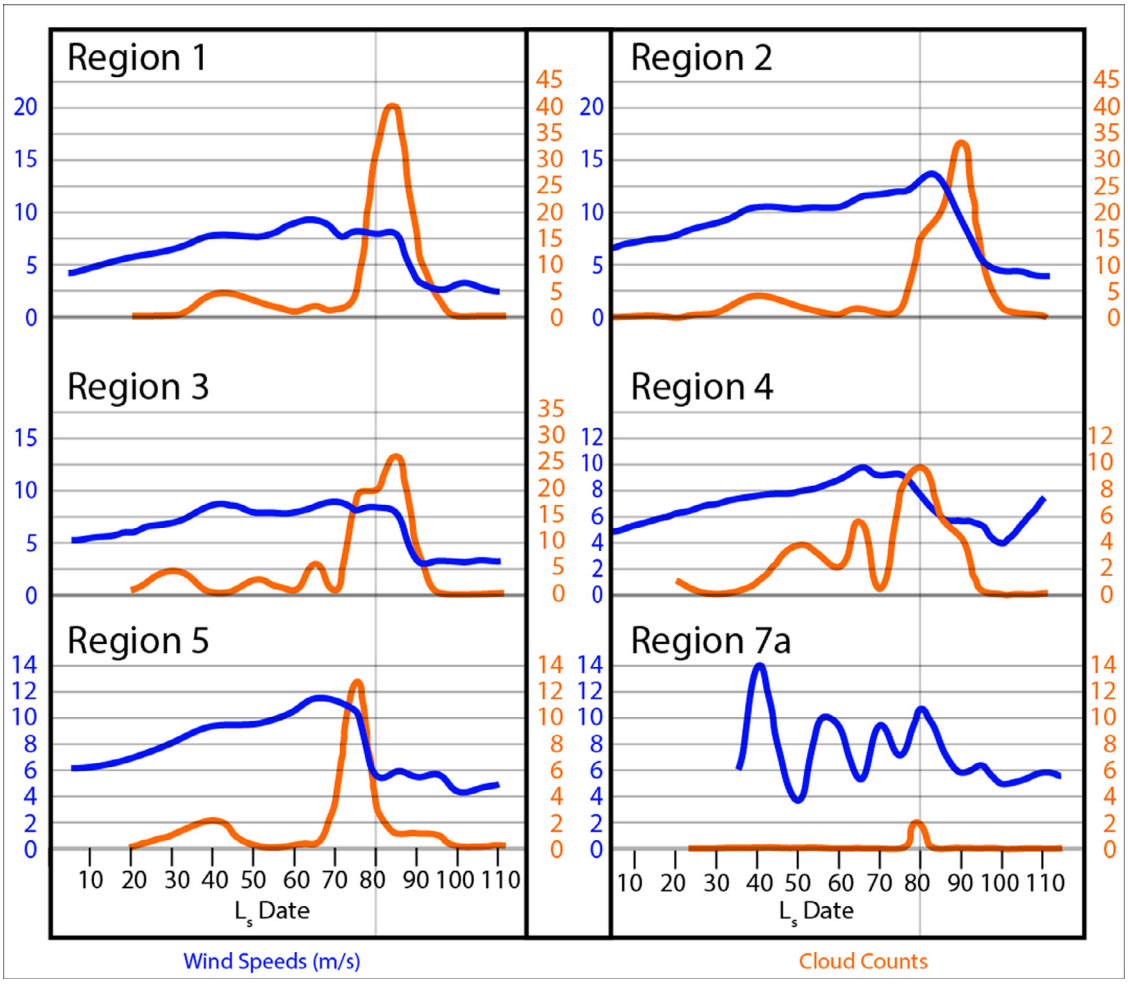

Fig. 5. Wind speeds and cloud counts for several regions defined in Fig. 3. Cloud counts peak at about the same time as wind speeds peak, sometimes with a delay. Cloud counts peak earlier in more southerly regions and later towards the north (Ls = 80° indicated to demonstrate timing delay in Regions 1–4. Region 5 clouds peak before Ls 80° Region 6 no longer exhibits spiral troughs, and no clouds form there. Region 7 has only two cloud detections that occur at Ls ~79°. Cloud are only counted from Mars Years 27 to 31.

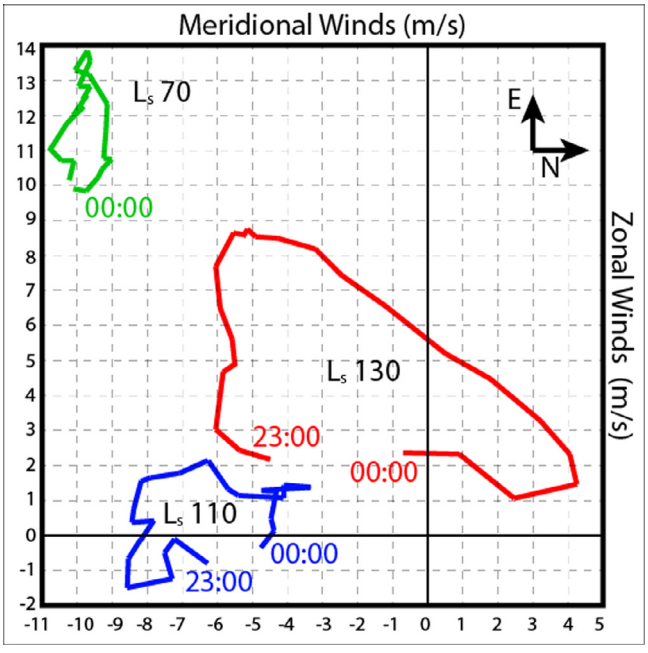

Fig. 6. Plots of wind directions for 24 hours at Location 4 (Fig. 3) for three dates. Winds are strongest before L_s 80° and have the greatest variability at L_s 130°. At L_s 70° the winds are more southwesterly, whereas at L_s 110° the winds are nearly due south during the entire day.

A slight time delay, however, can be detected between the wind speed drop and the cloud count drop. There are likely two reasons for this. First, the cloud counts are not perfect. They cover an entire region but sometimes have missing data points. This is because the THEMIS surveys were not uniform from year to year, and data gaps exist for downtime such as solar conjunction in March 2010 - or Ls ~60°–70° in Mars Year 30. We also do not include cloud counts from MY 32 or 33, which is considered as future work in order to improve statistics.

With that caveat in mind, we suggest that the primary cause of the slight delay in cloud count may be related to the atmospheric state not meeting the necessary requirements for making clouds. Super saturated water vapor is a necessary condition for clouds to form at katabatic jumps (Spiga and Smith, this issue). When the seasonal cap still covers the surface there is less water ice available to sublime and make vapor. Thus, the seasonal cap must retreat just poleward of a trough to maximize cloud potential, and the clouds can only form if two conditions are met: the seasonal cap has retreated sufficiently as to allow sublimation of water ice from the surface, and the winds are still near maximum speeds for the year, or slightly delayed after the CO_2 seasonal cap retreats past a specific location.

After the seasonal cap is gone for the summer, even when temperatures are warmer and the humidity is higher, the fast winds that form katabatic jumps are no longer present, and the cloud counts drop to zero. Supporting this interpretation,

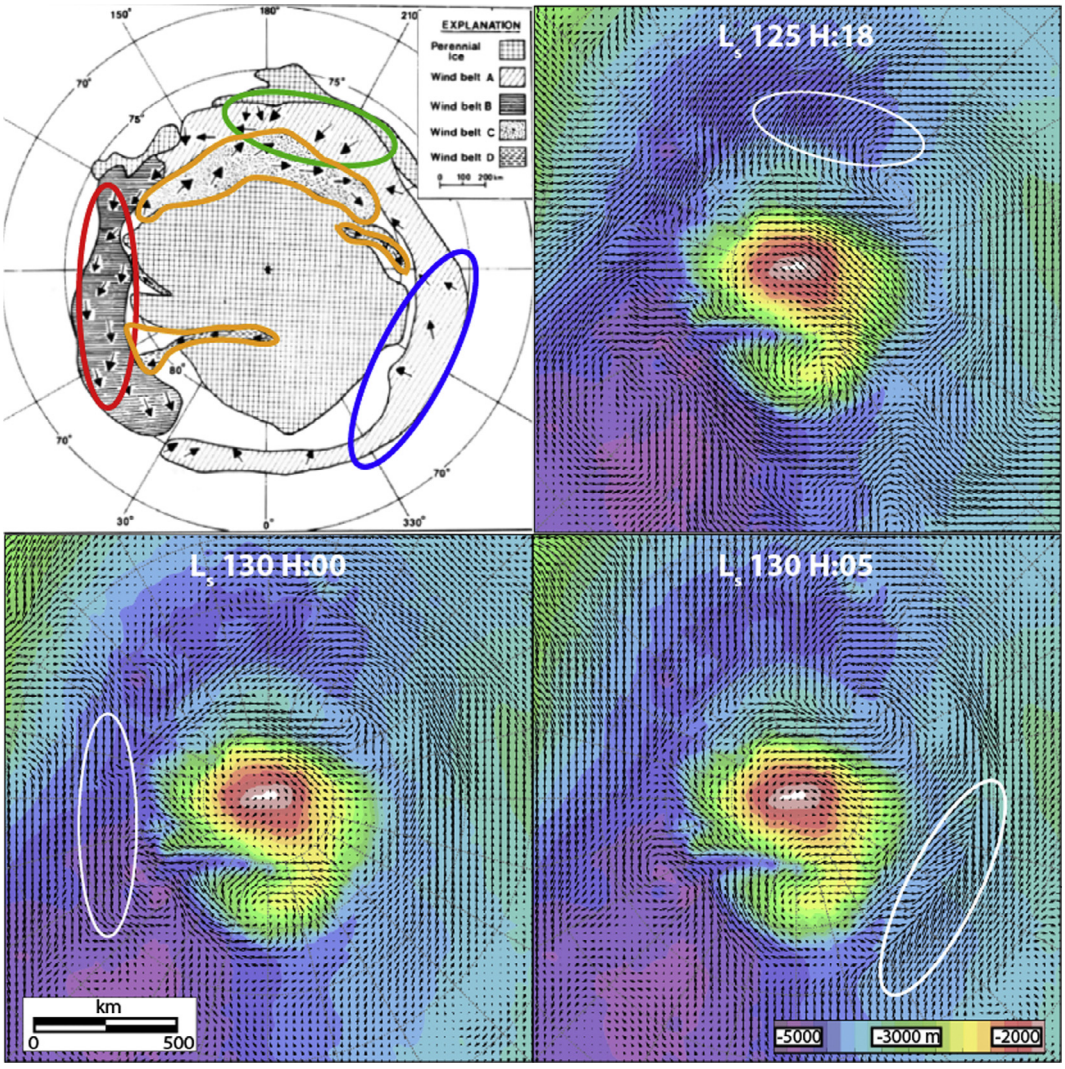

Fig. 7. Comparison of inferred dune migration (a) (Tsoar et al., 1999) to model outputs (b)–(d) Dune fields highlighted in orange align well to the modeled diurnal winds in spring, but other dune fields orient differently. (For interpretation of the references to colour in this figure legend, the reader is referred to the web version of this article.)

Smith et al. (2013) presented a histogram of all cloud counts per date (not separated by region) and found that the last clouds appeared around L_s 102° (in Mars Year 29), soon after the seasonal cap disappeared at L_s 95° (average over several years). The clouds did not return until around L_s 40° the following year.

Our finding regarding the link between variability of trough clouds and CO_2 seasonal cap retreat are similar to those for the southern pole (Smith et al., 2014), except that the NPLD covers a much smaller latitudinal range than the SPLD (80° to 90° vs. −73° to −90°). The lower latitude SPLD margins allow sublimation of water ice earlier in the respective spring, and clouds are found there earlier. Furthermore, the SPLD has a residual CO_2 cap that doesn't sublimate in summer, so two conditions needed to form clouds (enhanced winds that form katabatic jumps and availability of water vapor) persist throughout the summer until the seasonal cap returns. Thus, the SPLD clouds appear earlier in spring and persist throughout the summer.

We perform an initial comparison of wind directions for Location 4 at three dates (Fig. 6). This location is near to a region with non-parallel surface streaks, and we hypothesized that the streaks formed during different periods with distinct wind regimes. In this case the strongest winds were towards the southeast at L_s 70°, but another period of strong southerly winds formed at L_s 110°. At L_s 130° the winds were weaker but had more variability, even pointing north east during one part of the day. This preliminary analysis may prove useful for studying the dates that wind streaks form.

Past geomorphic studies of the winds in the north polar region included estimates of dune orientation and inferred wind speed (Tsoar et al., 1979; Massé et al., 2012) (Fig. 7). The Olympia Undae dune fields between 120° E and 240° E align closely to our modeled wind direction for the spring, and the timing of observed dune movement matches closely to the timing of maximum wind speeds in the same locations (Smith et al., 2016b). However, in other locations the observed dune migration does not match the generally southwest direction of springtime Coriolis steered winds. Therefore, if they are active they must be the result of winds that aren't dominant in the spring. Another factor may be polar transient enhancements of springtime winds (Tyler and Barnes, 2005) that don't develop in our short simulations.

We sought times during the year when strong winds paralleled the inferred wind directions of dune fields in each location and found that mid-summer had closer agreement than anytime in the spring (Fig. 7), but the winds are generally weaker than the springtime winds, and we don't have enough information to determine the actual sand flux. Future work is needed to perform a more systematic comparison between dune fields and mesoscale

wind regimes in the polar regions with an estimate of sand fluxes. This will help determine if the dune orientations are controlled by present processes or are remnants of older periods, perhaps when the obliquity was higher. In those epochs high latitude surface temperatures are warmer and the surface pressure is higher (Bierson et al., 2016; Phillips et al., 2011), so dune migration should have been more active.

5. Conclusion

In this study we produced a catalog of modeled diurnal winds from L_s 30° to L_s 140°, and qualitatively compared the wind speeds and transport availability of surface materials to inferred speeds and directions from observations. In general, we find that our modeled wind speeds do a good job of predicting when winds are most active on the surface and in what directions the winds move sediment.

For the trough clouds, modeled winds closely match the inferred maximum periods for polar wind strength and katabatic jumps, as evidenced by the seasonality in cloud formation. The clouds form when two conditions are met: when winds are fastest and when CO_2 ice does not cover the surface, permitting sublimation. These factors combine at different periods depending on which region of the NPLD is being studied. After the seasonal CO_2 cap retreats entirely, polar winds are not fast enough to meet those conditions, and trough cloud counts drop to zero.

Dune fields surround the NPLD, but modeled winds do not predict that each dune field migrates at the same time. Crest-lines in large dune fields between 120° E and 240° E align well with springtime katabatic winds that are steered by the Coriolis force, but dunes in other locations may be most active in mid-summer (L_s 125–130°) when diurnal winds match the inferred dune migration directions. Other possibilities are that they may be remnant fields indicating activity in a previous climate, or a compound dune morphology might be the expression of two wind regimes acting at different times in the year. Similar to the dunes, preliminary results indicate that throughout the season the diurnal winds may vary significantly in direction, potentially explaining non-parallel surface streaks on the NPLD.

Our simulations were for short, 3-day periods, which did not allow for transient synoptic structure to develop. That structure must play a role in mass transport at the surface and should be quantified with a more complete study including higher resolution simulations that cover larger regions and have longer durations. Only then will we be able to tell if synoptic structure reinforces some winds or steers the winds beyond what the diurnal temperature variations force. This will help us to determine which dune fields are active today, and which are relict from past states.

This was a first cut at modeling seasonal winds at high resolution across two seasons. Future work will aim to go beyond qualitative arguments and estimate the magnitude of material transport for dunes and spiral troughs. Specifically, we believe that a more advanced study, with higher resolution, greater coverage area, and longer durations will be able to answer the following geologic questions: (1) are the orientations of dunes near to the north pole dominated by the current wind regime, or do only the smaller ripples represent that regime; (2) what is the magnitude of material transport during a normal Mars day vs. a storm period for dunes; and (3) what effect do the katabatic winds have on current evolution of spiral troughs?

We also believe that a more advanced study will be able to characterize atmospheric circulation throughout the polar spring and summer, including large scale transients and the likelihood of storm formation. Some questions include: (1) what season(s) permit the formation of transient storms that spill to lower latitudes, (2) what is the duration of a storm, especially related to the transients, (3) what is the entire active season for katabatic winds, and how do transients enhance them to form clouds that affect spiral trough migration; and (4) what does late summer CO_2 deposition do to atmospheric circulation?

Acknowledgments

I. B. S. acknowledges support from the FrancoAmerican Fulbright Commission during a scientific visit at LMD (Paris) in 2014, which initiated this study. A.S. acknowledges funding from Centre National d'Études Spatiales (CNES).

Supplementary materials

Supplementary material associated with this article can be found, in the online version, at doi:10.1016/j.icarus.2017.10.005.

References

Bierson, C.J., Phillips, R.J., Smith, I.B., Wood, S.E., Putzig, N.E., Nunes, D., Byrne, S., 2016. Stratigraphy and evolution of the buried CO2 deposit in the Martian south polar cap. Geophys. Res. Lett. 43, 4172–4179. doi:10.1002/2016GL068457.

Bridges, N.T., Ayoub, F., Avouac, J.-P., Leprince, S., Lucas, A., Mattson, S., 2012. Earth-like sand fluxes on Mars. Nature 485, 339–342.

Brothers, T.C., Holt, J.W., Spiga, A., 2015. Planum Boreum basal unit topography, Mars: irregularities and insights from SHARAD. J. Geophys. Res. Planets 120, 1357–1375.

Brothers, T.C., Holt, J.W., Spiga, A., 2013. Orbital radar, imagery, and atmospheric modeling reveal an aeolian origin for Abalos Mensa, Mars. Geophys. Res. Lett. 40, 1334–1339. doi:10.1002/grl.50293.

Byrne, Shane, 2009. The polar deposits of Mars. Annu. Rev. Earth Planet Sci. 37, 8.1–8.26.

Calvin, W.M., Titus, T.N., 2008. Summer season variability of the north residual cap of Mars as observed by the Mars Global Surveyor Thermal Emission Spectrometer (MGS-TES). Planet. Space Sci. 56, 212–226. doi:10.1016/j.pss.2007.08.005.

Conway, S.J., Hovius, N., Barnie, T., Besserer, J., Le Mouélic, S., Orosei, R., Read, N.A., 2012. Climate-driven deposition of water ice and the formation of mounds in craters in Mars' north polar region. Icarus 220, 174–193. doi:10.1016/j.icarus.2012.04.021.

Ewing, R.C., Peyret, A.-P.B., Kocurek, G., Bourke, M., 2010. Dune field pattern formation and recent transporting winds in the Olympia Undae Dune Field, north polar region of Mars. J. Geophys. Res. Planets 1991–2012, 115.

Farmer, C.B., Doms, P.E., 1979. Global seasonal variation of water vapor on Mars and the implications for permafrost. J. Geophys. Res. Solid Earth 84, 2881–2888. doi:10.1029/JB084iB06p02881.

Fenton, L.K., Toigo, A.D., Richardson, M.I., 2005. Aeolian processes in Proctor Crater on Mars: mesoscale modeling of dune-forming winds. J. Geophys. Res. Planets 1991–2012, 110.

Fenton, L.K., Michaels, T.I., Chojnacki, M., Beyer, R.A., 2014. Inverse maximum gross bedform-normal transport 2: application to a dune field in Ganges Chasma, Mars and comparison with HiRISE repeat imagery and MRAMS. Icarus 230, 47–63.

Forget, F., Hourdin, F., Fournier, R., Hourdin, C., Talagrand, O., Collins, M., Lewis, S.R., Read, P.L., Huot, J.-P., 1999. Improved general circulation models of the Martian atmosphere from the surface to above 80 km. J. Geophys. Res. 104, 24155–24175. doi:10.1029/1999JE001025.

Hansen, C.J., Bourke, M., Bridges, N.T., Byrne, S., Colon, C., Diniega, S., Dundas, C., Herkenhoff, K., McEwen, A., Mellon, M., others, 2011. Seasonal erosion and restoration of Mars' northern polar dunes. Science 331, 575–578.

Hayne, P.O., Paige, D.A., Heavens, N.G., 2014. The role of snowfall in forming the seasonal ice caps of Mars: models and constraints from the Mars Climate Sounder. Icarus 231, 122–130.

Hayward, R.K., Mullins, K.F., Fenton, L.K., Hare, T.M., Titus, T.N., Bourke, M.C., Colaprete, A., Christensen, P.R., 2007. Mars global digital dune database and initial science results. J. Geophys. Res. Planets 1991–2012, 112.

Hayward, R.K., Titus, T.N., Michaels, T.I., Fenton, L.K., Colaprete, A., Christensen, P.R., 2009. Aeolian dunes as ground truth for atmospheric modeling on Mars. J. Geophys. Res. Planets 114, E11012. doi:10.1029/2009JE003428.

Holt, J.W., Fishbaugh, K.E., Byrne, S., Christian, S., Tanaka, K., Russell, P.S., Herkenhoff, K.E., Safaeinili, A., Putzig, N.E., Phillips, R.J., 2010. The construction of chasma boreale on Mars. Nature 465, 446–449.

Howard, A.D., 2000. The role of Eolian processes in forming surface features of the Martian polar layered deposits. Icarus 144, 267–288.

Howard, A.D., Cutts, J.A., Blasius, K.R., 1982. Stratigraphic relationships within Martian polar cap deposits. Icarus 50, 161–215.

Hvidberg, C.S., Fishbaugh, K.E., Winstrup, M., Svensson, A., Byrne, S., Herkenhoff, K.E., 2012. Reading the climate record of the Martian polar layered deposits. Icarus 221, 405–419. doi:10.1016/j.icarus.2012.08.009.

Koutnik, M.R., Byrne, S., Murray, B.C., Toigo, A.D., Crawford, Z.A., 2005. Eolian controlled modification of the Martian south polar layered deposits. Icarus 174, 490–501. doi:10.1016/j.icarus.2004.09.015.

Levrard, B., Forget, F., Montmessin, F., Laskar, J., 2007. Recent formation and evolution of northern Martian polar layered deposits as inferred from a Global Climate Model. J. Geophys. Res. 112, E06012.

Lied, N.T., 1964. Stationary hydraulic jumps in a katabatic flow near Davis, Antarctica, 1961.. *Aust. Meteor. Mag.* 47, 40–51.

Massé, M., Bourgeois, O., Le Mouélic, S., Verpoorter, C., Spiga, A., Le Deit, L., 2012. Wide distribution and glacial origin of polar gypsum on Mars. *Earth Planet. Sci. Lett.* 317–318, 44–55. doi:10.1016/j.epsl.2011.11.035.

Michaels, T.I., Rafkin, S.C.R., 2008. Meteorological predictions for candidate 2007 Phoenix Mars Lander sites using the Mars Regional Atmospheric Modeling System (MRAMS). J. Geophys. Res. Planets 1991–2012, 113.

Middlebrook, W.D., (2015). Three-Dimensional and Multi-Temporal Dune-Field Pattern Analysis in the Olympia Undae Dune Field, Mars (Thesis).

Pettré, P., André, J.C., 1991. Surface-pressure change through Loewe's phenomena and katabatic flow jumps- Study of two cases in Adelie Land, Antarctica. *J. Atmos. Sci.* 48, 557–571.

Phillips, R.J., Davis, B.J., Tanaka, K.L., Byrne, S., Mellon, M.T., Putzig, N.E., Haberle, R.M., Kahre, M.A., Campbell, B.A., Carter, L.M., Smith, I.B., Holt, J.W., Smrekar, S.E., Nunes, D.C., Plaut, J.J., Egan, A.F., Titus, T.N., Seu, R., 2011. Massive CO2 ice deposits sequestered in the south polar layered deposits of Mars. Science 332, 838–841. doi:10.1126/science.1203091.

Putzig, N.E., Phillips, R.J., Campbell, B.A., Holt, J.W., Plaut, J.J., Carter, L.M., Egan, A.F., Bernardini, F., Safaeinili, A., Seu, R., 2009. Subsurface structure of Planum Boreum from Mars Reconnaissance Orbiter shallow radar soundings. Icarus 204, 443–457.

Putzig, N.E., Mellon, M.T., Herkenhoff, K.E., Phillips, R.J., Davis, B.J., Ewer, K.J., Bowers, L.M., 2014. Thermal behavior and ice-table depth within the north polar erg of Mars. Icarus, *Third Planetary Dunes Systems* 230, 64–76. doi:10.1016/j.icarus.2013.07.010.

Rafkin, S.C., 2009. A positive radiative-dynamic feedback mechanism for the maintenance and growth of Martian dust storms. J. Geophys. Res. Planets 1991–2012, 114.

Siili, T., Haberle, R.M., Murphy, J.R., Savijarvi, H., 1999. Modelling of the combined late-winter ice cap edge and slope winds in Mars Hellas and Argyre regions. *Planet. Space Sci.* 47, 951–970. doi:10.1016/S0032-0633(99)00016-1.

Smith, D.E., Zuber, M.T., Neumann, G.A., 2001. Seasonal variations of snow depth on Mars. Science 294, 2141–2146. doi:10.1126/science.1066556.

Smith, I.B., Holt, J.W., 2010. Onset and migration of spiral troughs on Mars revealed by orbital radar. Nature 465, 450–453.

Smith, I.B., Holt, J.W., 2015. Spiral Trough Diversity on the North Pole of Mars, as Seen by SHARAD. J. Geophys. Res. Planets, 2014JE004720 doi:10.1002/2014JE004720.

Smith, I.B., Holt, J.W., Spiga, A., Howard, A.D., Parker, G., 2013. The spiral troughs of Mars as cyclic steps. J. Geophys. Res. Planets. doi:10.1002/jgre.20142.

Smith, I.B., Spiga, A., Holt, J.W., 2014. Aeolian processes as drivers of landform evolution at the South Pole of Mars. *Geomorphology*, Planetary Geomorphology: Proceedings of the 45th Annual Binghamton Geomorphology Symposium, held 12-14 September 2014 in Knoxville, Tennessee, USA, 240, pp. 54–69. doi:10.1016/j.geomorph.2014.08.026.

Smith, I.B., Putzig, N.E., Holt, J.W., Phillips, R.J., 2016a. An ice age recorded in the polar deposits of Mars. Science 352, 1075–1078. doi:10.1126/science.aad6968.

Smith, I.B., Spiga, A., Tyler, D., Ewing, R.C., 2016b. Wind at the north pole of Mars: comparisons of modeling and observations. In: 47th LPSC, p. 1632.

Spiga, A., Forget, F., 2009. A new model to simulate the Martian mesoscale and microscale atmospheric circulation: validation and first results. J. Geophys. Res. 114, E02009. doi:10.1029/2008JE003242.

Spiga, A., Forget, F., Madeleine, J.-B., Montabone, L., Lewis, S.R., Millour, E., 2011. The impact of martian mesoscale winds on surface temperature and on the determination of thermal inertia. Icarus 212, 504–519. doi:10.1016/j.icarus.2011.02.001.

Titus, T.N., 2005. Mars polar cap edges tracked over 3 full Mars years. In: 36th LPSC, p. 1993.

Toigo, A.D., Richardson, M.I., Wilson, R.J., Wang, H., Ingersoll, A.P., 2002. A first look at dust lifting and dust storms near the south pole of Mars with a mesoscale model. *J. Geophys. Res.* 107 4-4-13 10.1029/2001JE001592.

Tsoar, H., Greeley, R., Peterfreund, A.R., 1979. MARS: the North Polar Sand Sea and related wind patterns. J. Geophys. Res. Solid Earth 84, 8167–8180. doi:10.1029/JB084iB14p08167.

Tyler, D., Barnes, J.R., 2005. A mesoscale model study of summertime atmospheric circulations in the north polar region of Mars. J. Geophys. Res. Planets 1991–2012, 110.

Tyler, D., Barnes, J.R., 2014. Atmospheric mesoscale modeling of water and clouds during northern summer on Mars. Icarus 237, 388–414. doi:10.1016/j.icarus.2014.04.020.

Warner, N.H., Farmer, J.D., 2008. Importance of aeolian processes in the origin of the north polar chasmata, Mars. Icarus 196, 368–384.

Whiteway, J.A., Komguem, L., Dickinson, C., Cook, C., Illnicki, M., Seabrook, J., Popovici, V., Duck, T.J., Davy, R., Taylor, P.A., others, 2009. Mars water-ice clouds and precipitation. Science 325, 68.